



HAL
open science

Loss-tolerant parity measurement for distant quantum bits

Alain Sarlette, Mazyar Mirrahimi

► **To cite this version:**

Alain Sarlette, Mazyar Mirrahimi. Loss-tolerant parity measurement for distant quantum bits. 2016. hal-01395590v1

HAL Id: hal-01395590

<https://inria.hal.science/hal-01395590v1>

Submitted on 11 Nov 2016 (v1), last revised 14 Nov 2017 (v2)

HAL is a multi-disciplinary open access archive for the deposit and dissemination of scientific research documents, whether they are published or not. The documents may come from teaching and research institutions in France or abroad, or from public or private research centers.

L'archive ouverte pluridisciplinaire **HAL**, est destinée au dépôt et à la diffusion de documents scientifiques de niveau recherche, publiés ou non, émanant des établissements d'enseignement et de recherche français ou étrangers, des laboratoires publics ou privés.

Loss-tolerant parity measurement for distant quantum bits

Alain Sarlette^{1,2} and Mazyar Mirrahimi^{1,3}

¹*QUANTIC project-team, INRIA Paris, France*

²*Department of Electronics and Information Systems, Ghent University, Belgium*

³*Department of Applied Physics, Yale University, USA*

(Dated: July 23, 2016)

We propose a scheme to measure the parity of two distant qubits, while ensuring that losses on the quantum channel between them does not destroy coherences within the parity subspaces. This capability enables deterministic preparation of highly entangled qubit states whose fidelity is not limited by the transmission loss. The key observation is that for a probe electromagnetic field in a particular quantum state, namely a superposition of two coherent states of opposite phases, the transmission loss stochastically applies a near-unitary back-action on the probe state. This leads to a parity measurement protocol where the main effect of the transmission losses is a decrease in the measurement strength. By repeating the non-destructive (weak) parity measurement, one achieves a high-fidelity entanglement in spite of a significant transmission loss.

The correlation of distant systems through entanglement is a hallmark of quantum physics [1, 2] and plays a fundamental role in envisioned quantum technology. Most fundamentally, quantum teleportation [3] shows how entanglement is a resource for effectively transmitting the unknown state of a quantum system, without physically transmitting quantum states. Towards future quantum computers, such teleportation could transport information between few-qubits processing units, and memory units which must be well isolated and hence not directly coupled to the rest of the system via tunable physical interactions. This so-called modular architecture for quantum computing provides a viable solution to the major scaling problem for many-qubit quantum information processing [4, 5]. In quantum communication, similar ideas would allow quantum repeaters to purify information through local operations only, provided they can consume units of entanglement between the communicating devices [6, 7]; such quantum repeaters are a necessary technology for exploiting accurate quantum communication, with associated e.g. cryptographic benefits, over long distances.

A major challenge towards enabling these applications is that generating entangled states between distant systems must rely, itself, on a quantum channel [8]. Microwave experiments have demonstrated how to deterministically entangle separate quantum subsystems via parity measurements [9], yet with a fidelity directly limited by the quality of the quantum channel: any losses on the probe field imply losses in entanglement. Channel losses can also be made to affect preparation success probability, instead of preparation fidelity. Many theoretical proposals [10–14] and experiments [15–20] have considered high-fidelity entanglement generation, despite propagation losses, by heralding the preparation on some rare photo-detection events. The success rate of this probabilistic preparation is however usually very low. Furthermore, the preparation fidelity is still limited by imperfections such as dark counts of the photodetector.

The present letter solves this question with an explicit proposal for the essentially equivalent [8] achievement of *loss-tolerant* eigenstate-preserving quantum non-demolition (QND) parity measurement between spatially separated qubits. Our key idea is to transmit over the quantum channel particularly engineered quantum states of light, i.e. “cat states”, for which the dominant photon loss errors almost reduce to photon-number parity flips [21]. With this we design the interaction between qubits and probe field such that (i) measuring the probe at the output performs a QND measurement of qubits parity and (ii) photon loss events on the transmitted probe field render the detection less decisive (weak measurement) but affect only minimally the parity eigenstates. This measurement enables an efficient entanglement *stabilization* scheme, which not only generates highly entangled states but also protects them over arbitrarily long times against various noise channels.

The abstract setting (Fig.1a) comprises two target qubits $|q_A\rangle, |q_B\rangle$ at different locations A, B and possibly embedded in auxiliary quantum machinery, e.g. a cavity in circuit quantum electrodynamics (QED) setups [22]. For each measurement, a source generates a controlled “probe” quantum state $|\psi_p\rangle$ at A which then interacts with $|q_A\rangle$ according to a unitary U_A , is transmitted over a noisy quantum channel C , interacts with $|q_B\rangle$ according to U_B and finally hits a detector at B. Those probe states play the role of parity meter. Since the quantum channel is the unequivocal bottleneck for remote entanglement in state-of-the-art technology [23], we focus on this issue and assume in this letter that all (reasonable) local actions (i.e. U_A, U_B , generating $|\psi_p\rangle$, detection at B) are implemented perfectly. As we will show later, imperfections on such operations will have a small effect on steady state when we *stabilize* quantum entanglement via feedback.

The QND measurement of a quantum observable Q discriminates possibly imperfectly between the eigenspaces of Q , but ensures that every *eigenspace* of

Q remains unaffected for all possible detection results. When Q has degenerate eigenspaces, this only ensures that a state inside an eigenspace is sent to a state in the same eigenspace. An *Eigenstate-Preserving Quantum Non-Demolition* (EP-QND) measurement is a QND measurement that does not affect any *eigenstate* of Q . In other words, the EP-QND property ensures that the measurement acts as identity on each eigenspace [14]. Consider the parity observable $Q = Q_+ - Q_-$ for two qubits in the canonical basis $\{|0\rangle, |1\rangle\}$, with

$$Q_+ = |00\rangle\langle 00| + |11\rangle\langle 11|, \quad Q_- = |01\rangle\langle 01| + |10\rangle\langle 10|.$$

In a projective measurement of Q , detection result $+$ (resp. $-$) would project the two qubits onto the even parity manifold $\text{span}\{|00\rangle, |11\rangle\}$ (resp. the odd parity manifold $\text{span}\{|01\rangle, |10\rangle\}$). Less decisive EP-QND measurements can result for instance from classical detection uncertainty, e.g. with probability $1-\xi$ an even (resp. odd) parity state gives detection result $-$ (resp. $+$). Then the probability to detect \pm becomes $p_{\pm} = \xi\langle\psi|Q_{\pm}|\psi\rangle + (1-\xi)\langle\psi|Q_{\mp}|\psi\rangle$ with corresponding measurement back-action transforming initial state $|\psi\rangle$ into [24]

$$\tilde{\mathbb{K}}_{\pm}(|\psi\rangle\langle\psi|) = \frac{\xi Q_{\pm}|\psi\rangle\langle\psi|Q_{\pm} + (1-\xi)Q_{\mp}|\psi\rangle\langle\psi|Q_{\mp}}{p_{\pm}}.$$

Any even-parity (resp. odd-parity) state remains unchanged under such measurement back-action and predominantly gives detection result $+$ (resp. $-$), i.e. with probability $\xi \in (1/2, 1]$. By repeating the EP-QND measurement sufficiently often, a precise conclusion about parity can be obtained without disturbing any initial state of definite parity.

We first sketch our concept with $|\psi_p\rangle = |q_p\rangle$ a probe qubit. Starting with $|q_p\rangle = |0\rangle_p$ we let U_A (resp. U_B) implement a CNOT gate on $|q_p\rangle$ conditioned by $|q_A\rangle$ (resp. $|q_B\rangle$), see Fig.1b. If the channel C was perfect ($E_k = \text{Identity}$ for $k = 1, 2, \dots$ on Fig.1b), then an initial state $(|11\rangle \pm |00\rangle)_{A,B} |0\rangle_p / \sqrt{2}$ would remain unchanged, while an initial state $(|10\rangle \pm |01\rangle)_{A,B} |0\rangle_p / \sqrt{2}$ would become $(|10\rangle \pm |01\rangle)_{A,B} |1\rangle_p / \sqrt{2}$ just before detection of the probe. Thus the measurement operations correspond to $\tilde{\mathbb{K}}_+, \tilde{\mathbb{K}}_-$ with $\xi = 1$.

Now let the channel subject the probe to an unknown number $n \in \{0, 1, 2, \dots\}$ of bit-flips $E_k = |1\rangle\langle 0|_p + |0\rangle\langle 1|_p$; this can be represented as conditioning each bit-flip on an unknown hypothetical state of the environment. For n even, the outcome is as for the perfect channel. For n odd the final probe state is reversed, e.g. input $(|11\rangle \pm |00\rangle)_{A,B} |0\rangle_p / \sqrt{2}$ yields output $(|11\rangle \pm |00\rangle)_{A,B} |1\rangle_p / \sqrt{2}$, but most importantly, the target qubits' state remains unaffected. This essential property ensures that the expected evolution for n unknown (equivalently, tracing over the unknown states of the environment) remains an EP-QND parity measurement, explicitly described by op-

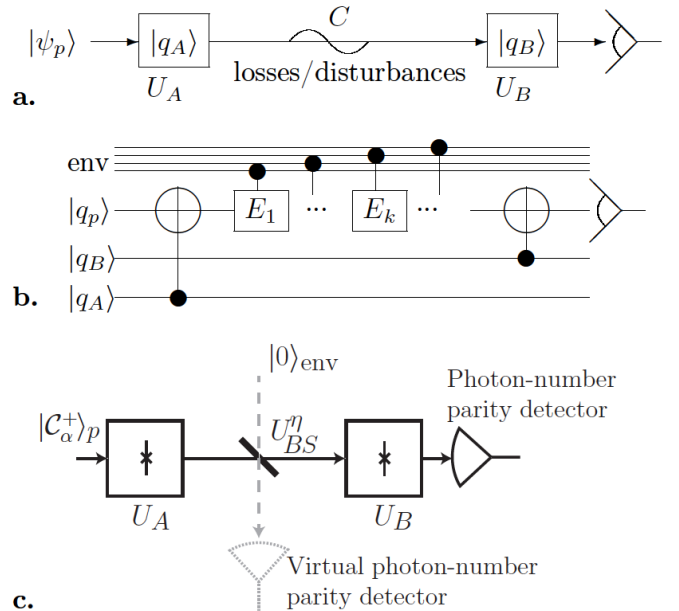


FIG. 1: **a.** General setup for remote parity measurement with a probe $|\psi_p\rangle$ propagating on a noisy quantum channel C between two target qubits $|q_A\rangle$ and $|q_B\rangle$. **b.** Quantum logic circuit summarizing our concept with CNOT gates involving target qubits $|q_A\rangle, |q_B\rangle$ and a probe qubit $|q_p\rangle$. We represent the unknown corrupting operations on the quantum channel as applying known $E_k, k = 1, 2, \dots$ conditionally on unknown states of the environment (env). **c.** Corresponding experimental setup with a probe field initialized in a coherent superposition of two opposite coherent states (“cat state”).

erators $\tilde{\mathbb{K}}_+, \tilde{\mathbb{K}}_-$ with $\xi = \sum_{n \text{ even}} \text{Proba}(n) < 1$. One can easily adapt this ξ to include detection misses and errors. A broad distribution of values of n implies low measurement contrast, pushing ξ close to $1/2$, but it does not impede its EP-QND character. Hence when sufficiently many measurements can be repeated within a relevant timescale, a conclusive result is obtained even for ξ close to $1/2$ (see details below).

This EP-QND property is lost under general channel errors. If for instance C includes a phase-flip $E_1 = |0\rangle\langle 0| - |1\rangle\langle 1|_p$, then the initial even-parity Bell state $|\psi_+\rangle = (|11\rangle + |00\rangle)_{A,B} / \sqrt{2}$ gets transformed by measurement back-action into $|\psi_-\rangle = (|11\rangle - |00\rangle)_{A,B} / \sqrt{2}$; thus this eigenstate of Q is not conserved, breaking the EP-QND character. Not knowing if E_1 was applied or not, the initial maximally entangled state $|\psi_+\rangle$ gets transformed into a statistical mixture of $|\psi_+\rangle$ and $|\psi_-\rangle$, i.e. entanglement is lost. In fact it is impossible to ensure EP-QND parity measurement when the channel disturbance can be arbitrary [8].

These abstract properties indicate a pathway towards loss-tolerant parity measurement: use a subspace of probe states on which the dominant decoherence channel acts as a unitary root of identity, e.g. a bit-flip. Our key observation is that this fits a physical implementa-

tion where the probe is an electromagnetic field pulse whose logical states are materialized by so-called “cat states”, i.e. mesoscopic superpositions of coherent states. This encoding, proposed earlier for quantum computing [21, 25], ensures that photon losses imply in good approximation, coherent logical bit flips. The rest of this letter describes such implementation in detail.

This physical implementation of loss-tolerant parity measurement is sketched in Figure 1c. We denote

$$\left| \mathcal{C}_\beta^\pm \right\rangle = (|\beta\rangle \pm |-\beta\rangle) / \mathcal{N}_\beta^\pm, \quad \mathcal{N}_\beta^\pm = \sqrt{2 \pm 2 e^{-2|\beta|^2}},$$

the superpositions between two coherent states $|\beta\rangle$ and $|-\beta\rangle$, $\beta \in \mathbb{R}$; the normalization constants \mathcal{N}_β^\pm rapidly approach $\sqrt{2}$ as the coherent amplitude β increases. The probe field is initially prepared in $|\mathcal{C}_\alpha^+\rangle_p$ and interacts with two qubit-cavity systems in a cascaded manner. Between the two setups it is exposed to losses, modeled as mixing with the vacuum state $|0\rangle_{\text{env}}$ of an ancillary mode through a beam-splitter unitary operator U_{BS}^η with transmittance $\sqrt{\eta}$ and reflectance $\sqrt{1-\eta}$. The unitary operators apply:

$$\begin{aligned} U_A |0\rangle_A |\mathcal{C}_\alpha^\pm\rangle_p &= |0\rangle_A |\mathcal{C}_\alpha^\pm\rangle_p, \quad U_A |1\rangle_A |\mathcal{C}_\alpha^\pm\rangle_p = |1\rangle_A |\mathcal{C}_\alpha^\mp\rangle_p, \\ U_B |0\rangle_B |\mathcal{C}_{\sqrt{\eta}\alpha}^\pm\rangle_p &= |0\rangle_B |\mathcal{C}_{\sqrt{\eta}\alpha}^\pm\rangle_p, \\ U_B |1\rangle_B |\mathcal{C}_{\sqrt{\eta}\alpha}^\pm\rangle_p &= |1\rangle_B |\mathcal{C}_{\sqrt{\eta}\alpha}^\mp\rangle_p, \\ U_{\text{BS}}^\eta |\mathcal{C}_\alpha^\pm\rangle_p |0\rangle_{\text{env}} &= \\ & \frac{1}{\mathcal{N}_\alpha^\pm} \left(|\sqrt{\eta}\alpha\rangle_p |\sqrt{1-\eta}\alpha\rangle_{\text{env}} \pm |-\sqrt{\eta}\alpha\rangle_p |-\sqrt{1-\eta}\alpha\rangle_{\text{env}} \right). \end{aligned} \quad (1)$$

Finally, after interaction with the second qubit, a measurement projects the probe’s state onto $|\mathcal{C}_{\sqrt{\eta}\alpha}^+\rangle_p$ or $|\mathcal{C}_{\sqrt{\eta}\alpha}^-\rangle_p$. Identifying $|\mathcal{C}_\beta^+\rangle_p$ and $|\mathcal{C}_\beta^-\rangle_p$ respectively with logical $|0\rangle_p$ and $|1\rangle_p$, we recover the scheme where U_A, U_B implement CNOT gates.

We now analyze the performance of this scheme. As we trace on the ancillary field modeling the losses, we can without loss of generality imagine a virtual detector also projecting it to $|\mathcal{C}_{\sqrt{1-\eta}\alpha}^+\rangle_{\text{env}}$ or $|\mathcal{C}_{\sqrt{1-\eta}\alpha}^-\rangle_{\text{env}}$, but with unread detection result. The measurement outcomes of the two detectors (one real and one virtual) are associated to four Kraus operators $M_{\sigma,\sigma}$ and $M_{\sigma,-\sigma}$ with $\sigma \in \{+, -\}$, modeling the back-action of the measurements on the target qubits: e.g. their state ρ , after measuring even parities for both detectors, is modified to $M_{+,+}\rho M_{+,+}^\dagger / \text{Tr}(M_{+,+}\rho M_{+,+}^\dagger)$. Following the computations of the supplementary material, these Kraus op-

erators are

$$\begin{aligned} M_{\sigma,\sigma} &= \frac{\mathcal{N}_{\sqrt{1-\eta}\alpha}^\sigma}{2} \left(\frac{\mathcal{N}_{\sqrt{\eta}\alpha}^\sigma}{\mathcal{N}_\alpha^+} |00\rangle \langle 00| + \frac{\mathcal{N}_{\sqrt{\eta}\alpha}^{(-\sigma)}}{\mathcal{N}_\alpha^-} |11\rangle \langle 11| \right) \\ M_{\sigma,-\sigma} &= \frac{\mathcal{N}_{\sqrt{1-\eta}\alpha}^{(-\sigma)}}{2} \left(\frac{\mathcal{N}_{\sqrt{\eta}\alpha}^\sigma}{\mathcal{N}_\alpha^-} |10\rangle \langle 10| + \frac{\mathcal{N}_{\sqrt{\eta}\alpha}^{(-\sigma)}}{\mathcal{N}_\alpha^+} |01\rangle \langle 01| \right). \end{aligned} \quad (2)$$

Discarding the inaccessible outcome of the virtual detector, the back-action induced by the probe field measurement follows:

$$\begin{aligned} \mathbb{K}_+(\rho) &= \frac{M_{+,+}\rho M_{+,+}^\dagger + M_{+,-}\rho M_{+,-}^\dagger}{\text{Tr}(M_{+,+}\rho M_{+,+}^\dagger + M_{+,-}\rho M_{+,-}^\dagger)}, \\ \mathbb{K}_-(\rho) &= \frac{M_{-,+}\rho M_{-,+}^\dagger + M_{-,-}\rho M_{-,-}^\dagger}{\text{Tr}(M_{-,+}\rho M_{-,+}^\dagger + M_{-,-}\rho M_{-,-}^\dagger)}. \end{aligned} \quad (3)$$

In the lossless case ($\eta = 1$), $M_{+,-}$ and $M_{-,-}$ vanish as $\mathcal{N}_0^- = 0$; the coefficients in front of $|00\rangle \langle 00|$ and $|11\rangle \langle 11|$ in $M_{+,+}$ and in front of $|01\rangle \langle 01|$ and $|10\rangle \langle 10|$ in $M_{-,+}$ are identical, equal to 1. This is a projective parity measurement, as described by $\tilde{\mathbb{K}}_+, \tilde{\mathbb{K}}_-$ with $\xi = 1$.

The effect of transmission losses ($\eta < 1$) is twofold. First, it reduces the measurement strength. Indeed, when the probe field is detected in a given parity (e.g. +), the qubits could be projected to the opposite parity (e.g. by Kraus operator $M_{+,-}$). However, each measurement does increase the conditional probability of finding the qubits in the same parity as the one indicated by the detections, because $\mathcal{N}_{\sqrt{1-\eta}\alpha}^+ \min\left(\frac{\mathcal{N}_{\sqrt{\eta}\alpha}^+}{\mathcal{N}_\alpha^+}, \frac{\mathcal{N}_{\sqrt{\eta}\alpha}^-}{\mathcal{N}_\alpha^-}\right) > \mathcal{N}_{\sqrt{1-\eta}\alpha}^- \max\left(\frac{\mathcal{N}_{\sqrt{\eta}\alpha}^+}{\mathcal{N}_\alpha^+}, \frac{\mathcal{N}_{\sqrt{\eta}\alpha}^-}{\mathcal{N}_\alpha^-}\right)$. A projective parity measurement under perfect transmission ($\eta = 1$) is thus replaced by a less decisive measurement for $\eta < 1$, where at each shot we gain partial information on the parity. By repeating the measurement the state gets projected onto a well-defined parity subspace. An initial state of definite parity always keeps this parity (e.g. $M_{+,-}(|00\rangle + |11\rangle) = 0$).

The second, more harmful effect of transmission loss is a slight perturbation of the EP-QND property, by introducing slow mixing within each parity subspace. This is due to the coherent states $|\beta\rangle$ and $|-\beta\rangle$ not being perfectly orthogonal, so that $\mathcal{N}_\beta^+ \neq \mathcal{N}_\beta^-$. This effectively induces dephasing inside parity subspaces, e.g. $\frac{\mathcal{N}_{\sqrt{\eta}\alpha}^+}{\mathcal{N}_\alpha^+} > \frac{\mathcal{N}_{\sqrt{\eta}\alpha}^-}{\mathcal{N}_\alpha^-}$ implies that $M_{+,+}$ drives $|B_\pm^e\rangle = (|00\rangle \pm |11\rangle)/\sqrt{2}$ towards $|00\rangle = (|B_+^e\rangle + |B_-^e\rangle)/\sqrt{2}$, while $M_{-,-}$ would drive them towards $|11\rangle = (|B_+^e\rangle - |B_-^e\rangle)/\sqrt{2}$.

Simulations on Fig. 2a illustrate the competition between parity measurement and undesired dephasing for various $|\alpha|^2$ (average number of photons in the probe field). Initializing both qubits in the state $|+X\rangle = (|0\rangle + |1\rangle)/\sqrt{2}$, an EP-QND parity measurement should

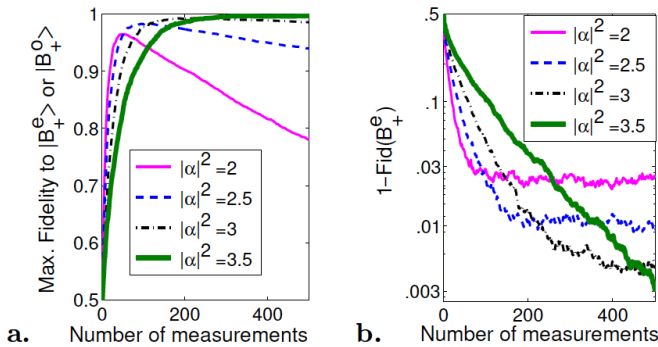


FIG. 2: **a.** Average evolution, over 1000 Monte-Carlo simulations, of the initial state $(|0\rangle + |1\rangle)_A(|0\rangle + |1\rangle)_B/2$ under repeated approximate EP-QND parity measurements (2),(3), for various probe field intensities $|\alpha|^2$ and transmission efficiency $\eta = .75$. The state initially converges towards a definite parity state $|B_+^e\rangle = (|00\rangle + |11\rangle)/\sqrt{2}$ or $|B_+^o\rangle = (|01\rangle + |10\rangle)/\sqrt{2}$ thanks to the measurement, then slowly loses fidelity to those states by dephasing, due to the slight perturbation of the EP-QND property inside definite parity subspaces. **b.** The dephasing can be counteracted by adding a simple feedback scheme (see main text), hence stabilizing $|B_+^e\rangle$ with high fidelity $Fid(B_+^e) = \langle B_+^e | \rho | B_+^e \rangle$.

project the joint state towards one of the two Bell states $|B_+^e\rangle = (|00\rangle + |11\rangle)/\sqrt{2}$ or $|B_+^o\rangle = (|01\rangle + |10\rangle)/\sqrt{2}$. This is the dominant tendency on Fig. 2(a), but transmission loss induces slow dephasing, mixing the target Bell states with the undesired ones $|B_-^e\rangle = (|00\rangle - |11\rangle)/\sqrt{2}$ and $|B_-^o\rangle = (|01\rangle - |10\rangle)/\sqrt{2}$. By increasing $|\alpha|^2$, this undesired dephasing gets suppressed significantly, at the expense of slower convergence, i.e. weaker parity measurement. As soon as $\eta > 1/2$, one can achieve arbitrarily high fidelity in this way.

This near EP-QND parity measurement can be used to stabilize a particular Bell state with a simple feedback protocol. To stabilize $|B_+^e\rangle$, (i) apply a π -pulse around the X -axis on the first qubit whenever the measurements estimate a probability higher than 1/2 to be in the odd parity subspace, (ii) after that, apply a $\pi/2$ -pulse on both qubits around the Y -axis irrespectively of the detection result. The measurement back-action favors convergence towards the dominant parity, the π pulse correcting the parity whenever this is not even. This pushes the state towards the span of $|B_+^e\rangle, |B_-^e\rangle$ without favoring the target $|B_+^e\rangle$. The two $\pi/2$ -pulses then leave $|B_+^e\rangle$ untouched and send the undesired $|B_-^e\rangle$ onto $|B_+^o\rangle$, such that the next parity measurement stochastically moves the corresponding population as well towards the target. Simulations on Fig. 2b illustrate the performance of this protocol, having fixed $\eta = .75$ and varying $|\alpha|^2$. Feedback stabilization of entanglement is further discussed in the supplementary material [8].

Convergence rates per measurement iteration can be calculated analytically for both the parity measurement

and the spurious dephasing, yielding respectively [8]:

$$r_{\text{parity}} = \frac{1}{2} \log \left(\frac{1 - e^{-4|\alpha|^2}}{1 - e^{-4(1-\eta)|\alpha|^2}} \right),$$

$$r_{\text{dephasing}} = \frac{1}{2} \log \left(\frac{1 - e^{-4|\alpha|^2}}{1 - e^{-4\eta|\alpha|^2}} \right).$$

This allows to estimate the measurement performance as a function of η and $|\alpha|^2$. Consider again the evolution depicted on Fig. 2a. The fidelity to the closest Bell state is 1/2 times the sum of two terms: dominant parity population, which converges from 1/2 to 1 at roughly a rate r_{parity} , and dominant phase population, which decreases from 1 to 1/2 at a rate $r_{\text{dephasing}}$. The two terms contribute equally to the error after a number of measurements $\tau = \tau_{\text{meas}}$ satisfying $e^{-r_{\text{parity}}\tau} + e^{-r_{\text{dephasing}}\tau} = 1$. The corresponding estimate of Bell state fidelity is $F_{\text{meas}} = 1 - e^{-r_{\text{parity}}\tau_{\text{meas}}}/2$. Figure 3 illustrates these estimates of our parity measurement's performance. For transmission efficiency as low as 70% we can get F_{meas} as high as 99% in 400 measurement runs, taking $|\alpha|^2 = 3.273$. Increasing η to 85% one achieves the same F_{meas} with only 17 measurements, taking $|\alpha|^2 = 1.63$.

Returning to the feedback stabilization, the convergence rate will be of order r_{parity}/T_d , where T_d is the duration of a single measurement iteration. As soon as this rate dominates the inherent decoherence rate $1/T_2$ of the qubits, high-fidelity entanglement can be preserved over arbitrary long times. Note that after tracing out the probe fields, the effect of imprecise operations in the protocol can be modeled by additional error channels on the qubits. These can be put on the same footing as inherent T_2 and will thus also be compensated by the stabilization (see [8]).

All the required operations for this proposal have been individually implemented within the framework of quantum superconducting circuits. The strong dispersive coupling of a transmon qubit to a high-Q cavity mode [26], provides universal controllability of the state of the quantum harmonic oscillator modeling the cavity mode [27, 28]. This controllability has been experimentally illustrated with circuit QED setups [29, 30]. Such a coupling enables to prepare the probe field in a cat state and to perform the CNOT gates U_A and U_B of (1) between the qubits and associated intra-cavity fields. Recent experiments realizing a variable coupling between cavity modes and a transmission line [31–33], provide the possibility of catching the propagating microwave field, performing the required gate between the qubit and the cavity field, and finally releasing back the cavity photons. Finally, while the measurement of photon-number parity has also been realized in a similar setup [34], one can further simplify the protocol by letting U_B map the intra-cavity field to coherent states $|\pm\sqrt{\eta}\alpha\rangle$ instead of

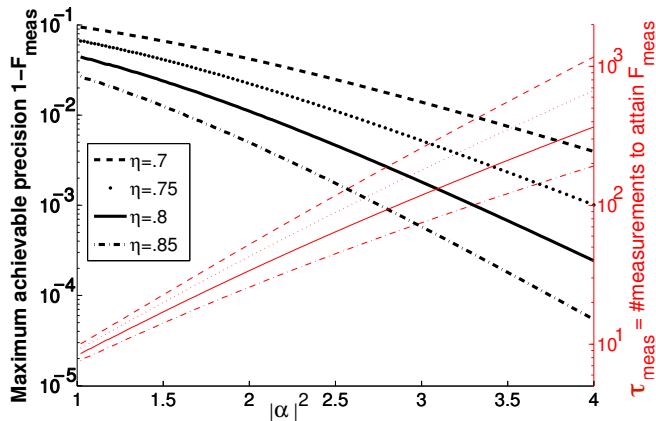


FIG. 3: (thick black, left axis) Estimate F_{meas} of the highest fidelity to the closest Bell state, obtained by repeated application of our near EP-QND parity measurement (2),(3) starting from $(|0\rangle + |1\rangle)_A(|0\rangle + |1\rangle)_B/2$, before dephasing destroys coherence in absence of feedback; (thin red, right axis) Estimate τ_{meas} of the number of measurements after which this highest fidelity is reached, giving an indication of measurement strength.

the cat states $|\mathcal{C}_{\sqrt{\eta}\alpha}^{\pm}\rangle$. This would allow to replace a photon-number parity measurement by a simple homodyne detection of the released field using a parametric amplifier [35]. A single measurement duration in such experimental realization depends mainly on the time required to perform the operations U_A and U_B . As explained in [27, 28] this gate time is roughly the inverse of the dispersive coupling strength. Recent experiments where this coupling strength is more than three orders of magnitude larger than both the qubit and the cavity decay rates [29, 30, 36] indicate that high entanglement fidelities should be achievable whenever a transmission efficiency of more than 70% is reached.

We have shown that it is possible to perform a near EP-QND measurement of the parity of two distant qubits despite an important loss through the transmission channel between them. By preparing the probe field in a quantum superposition of two coherent states with opposite phases, we avoid any back-action of the probe losses on the target qubits' state inside any parity subspace. Indeed, such losses mainly decrease the measurement strength but barely affect its EP-QND character. Therefore, even with an inefficient transmission channel, by repeating the measurement many times one efficiently projects the joint qubits state onto a definite parity subspace. This enables not only to deterministically and hardware-efficiently prepare an entangled state of two distant qubits, but combined with a quantum feedback strategy it also protects such state against decoherence channels and systematic errors. The operations required to perform this loss-tolerant parity measurement are within the reach of state of the art experiments. Their

implementation will lead to an important step forward for implementing quantum teleportation protocols in a loss-tolerant way, and more particularly towards the modular architecture solution for large scale quantum information processors [4].

The authors thank the Agence Nationale de la Recherche for financial support under grant ANR-14-CE26-0018.

-
- [1] J. Bell, *Physics* **1**, 195 (1964).
 - [2] A. Aspect, P. Grangier, and G. Roger, *Phys. Rev. Lett.* **47**, 460 (1981).
 - [3] C. Bennett, G. Brassard, C. Crépeau, R. Jozsa, A. Peres, and W. Wootters, *Phys. Rev. Lett.* **70**, 1895 (1993).
 - [4] M. Devoret and R. Schoelkopf, *Science* **339**, 1169 (2013).
 - [5] C. Monroe, R. Raussendorf, A. Ruthven, K. Brown, P. Maunz, L.-M. Duan, and J. Kim, *Phys. Rev. A* **89**, 022317 (2014).
 - [6] H.-J. Briegel, W. Dür, J. Cirac, and P. Zoller, *Phys. Rev. Lett.* **81**, 5932 (1998).
 - [7] L.-M. Duan, M. Lukin, J. Cirac, and P. Zoller, *Nature* **414**, 413 (2001).
 - [8] *See the supplementary material.*
 - [9] N. Roch, M. Schwartz, F. Motzoi, C. Macklin, R. Vijay, A. Eddins, A. Korotkov, K. Whaley, M. Sarovar, and I. Siddiqi, *Phys. Rev. Lett.* **112**, 170501 (2014).
 - [10] S.D. Barrett and P. Kok, *Phys. Rev. A* **71**, 060310 (2005).
 - [11] C. Cabrillo, J.I. Cirac, P. García-Fernández, and P. Zoller, *Phys. Rev. A* **59**, 1025 (1999).
 - [12] L. Jiang, J.M. Taylor, A.S. Soerensen, and M.D. Lukin, *Int. J. Quant. Inf.* **8(01n02)**, 93 (2010).
 - [13] T.D. Ladd, P. van Loock, K. Nemoto, W.J. Munro, and Y. Yamamoto, *New J. Phys.* **8**, 184 (2006).
 - [14] E.T. Campbell, *Phys. Rev. A (Rapid Comm)* **76**, 040302 (2007).
 - [15] C. Chou, H. de Riedmatten, D. Felinto, S. Polyakov, S. van Enk, and H. Kimble, *Nature* **438**, 828 (2005).
 - [16] D. Moehring, P. Maunz, S. Olmschenk, K. Younge, D. Matsukevich, L.-M. Duan, and C. Monroe, *Nature* **449**, 68 (2007).
 - [17] A. Ourjoumtsev, F. Ferreyrol, R. Tualle-Brouiri, and P. Grangier, *Nature Physics* **5**, 189 (2009).
 - [18] J. Hofmann, M. Krug, N. Ortegel, L. Gérard, M. Weber, W. Rosenfeld, and H. Weinfurter, *Science* **337**, 72 (2012).
 - [19] H. Bernien, B. Hensen, W. Pfaff, G. Koolstra, M. Blok, L. Robledo, T. Tamini, M. Markham, D. Twitchen, L. Childress, et al., *Nature* **497**, 86 (2013).
 - [20] A. Narla, S. Shankar, M. Hatridge, Z. Leghtas, K. Sliwa, E. Zaly-Geller, S. Mundhada, W. Pfaff, L. Frunzio, R. Schoelkopf, et al., arXiv:1603.03742 (2016).
 - [21] Z. Leghtas, G. Kirchmair, B. Vlastakis, R. Schoelkopf, M. Devoret, and M. Mirrahimi, *Phys. Rev. Lett.* **111** (2013).
 - [22] A. Wallraff, D. Schuster, A. Blais, L. Frunzio, R. Huang, J. Majer, S. Kumar, S. Girvin, and R. Schoelkopf, *Nature* **431**, 162 (2004).
 - [23] K. Lalumière and A. Blais, *Physics* **7**, 45 (2014).
 - [24] M. Nielsen and I. Chuang, *Quantum Computation and Quantum Information* (Cambridge University Press,

- 2000).
- [25] M. Mirrahimi, Z. Leghtas, V. Albert, S. Touzard, R. Schoelkopf, L. Jiang, and M. Devoret, *New J. of Physics* **16**, 045014 (2014).
 - [26] D. Schuster, A. Houck, J. Schreier, A. Wallraff, J. Gambetta, A. Blais, L. Frunzio, J. Majer, B. Johnson, M. Devoret, et al., *Nature* **445**, 515 (2007).
 - [27] Z. Leghtas, G. Kirchmair, B. Vlastakis, M. Devoret, R. Schoelkopf, and M. Mirrahimi, *Phys. Rev. A* **87** (2013).
 - [28] S. Krastanov, V. Albert, C. Shen, C.-L. Zou, R. Heeres, B. Vlastakis, R. Schoelkopf, and L. Jiang, *Phys. Rev. A* **92**, 040303 (2015).
 - [29] B. Vlastakis, G. Kirchmair, Z. Leghtas, S. Nigg, L. Frunzio, S. Girvin, M. Mirrahimi, M. Devoret, and R. Schoelkopf, *Science* **342**, 607 (2013).
 - [30] R. Heeres, B. Vlastakis, E. Holland, S. Krastanov, V. Albert, L. Frunzio, L. Jiang, and R. Schoelkopf, *Phys. Rev. Lett.* **115**, 137002 (2015).
 - [31] Y. Yin, Y. Chen, D. Sank, P. O'Malley, T. White, R. Barends, J. Kelly, E. Lucero, M. Mariantoni, A. Megrant, et al., *Phys. Rev. Lett.* **110**, 107001 (2013).
 - [32] J. Wenner, Y. Yin, Y. Chen, R. Barends, B. Chiaro, E. Jeffrey, J. Kelly, A. Megrant, J. Mutus, C. Neill, et al., *Phys. Rev. Lett.* **112**, 210501 (2014).
 - [33] E. Flurin, N. Roch, J. Pillet, F. Mallet, and B. Huard, *Phys. Rev. Lett.* **114**, 090503 (2015).
 - [34] L. Sun, A. Petrenko, Z. Leghtas, B. Vlastakis, G. Kirchmair, K. Sliwa, A. Narla, M. Hatridge, S. Shankar, J. Blumoff, et al., *Nature* **511**, 444 (2014).
 - [35] R. Vijay, M. Devoret, and I. Siddiqi, *Rev. Sci. Instrum.* **80**, 111101 (2009).
 - [36] H. Paik, D. Schuster, L. Bishop, G. Kirchmair, G. Catelani, A. Sears, B. Johnson, M. Reagor, L. Frunzio, L. Glazman, et al., *Phys. Rev. Lett.* **107**, 240501 (2011).
 - [37] P. Rouchon, *Automatic Control*, *IEEE Transactions on* **56**, 2743 (2011).